CCK-2/Gastrin Receptor–Targeted Tumor Imaging with ^{99m}Tc-Labeled Minigastrin Analogs

Berthold A. Nock, PhD[1]; Theodosia Maina, PhD[1]; Martin Béhé, PhD[2]; Anastasia Nikolopoulou, MSci[1]; Martin Gotthardt, MD[2]; Jörg S. Schmitt, PhD[3]; Thomas M. Behr, MD[2]; and Helmut R. Mäcke, PhD[3]

[1]Institute of Radioisotopes–Radiodiagnostic Products, National Center for Scientific Research Demokritos, Athens, Greece; [2]Department of Nuclear Medicine, Philipps University Marburg, Marburg, Germany; and [3]Division of Radiological Chemistry, University Hospital Basel, Basel, Switzerland

The aim of this study was to evaluate 3 new ^{99m}Tc-labeled minigastrin analogs modified with open chain tetraamines at the N-terminus for their suitability in the CCK-2/gastrin-R–targeted imaging of tumors (CCK-2/gastrin-R = cholecystokinin subtype 2/gastrin receptor). **Methods:** The [(D)Glu[1]]minigastrin sequence was assembled on the solid support and the respective tetraamine precursors coupled at the N-terminus. Purified peptide conjugates were labeled with ^{99m}Tc under alkaline conditions. Saturation binding experiments were performed for (radio)metallated peptides [^{99m}Tc/^{99g}Tc]Demogastrin 1–3 in rat acinar pancreatic AR4-2J cell membranes. Internalization was studied in AR4-2J cells at 37°C. Radiopeptide stability was tested in murine plasma, urine, and kidney homogenates. Tissue distribution of the peptides was compared in healthy mice and athymic mice bearing AR4-2J tumors. **Results:** Peptide conjugates were obtained in 10%–30% overall yields by solid-phase techniques. Radiolabeling afforded >98% pure [^{99m}Tc]Demogastrin 1–3 species in specific activities of ~37 GBq/μmol. Radiopeptides retained a high affinity for the CCK-2/gastrin-R in vitro (50% inhibitory concentration values of ~1 nmol/L) and internalized rapidly in CCK-2/gastrin-R–positive cells. After injection in mice they displayed rapid, high, and specific localization in the CCK-2/gastrin-R–expressing tissues (stomach and AR4-2J tumor) and were excreted from the body via the kidneys in the form of hydrophilic metabolites. **Conclusion:** The promising characteristics of [^{99m}Tc]Demogastrin 1–3 both in vitro and in animal models illustrate their suitability for CCK-2/gastrin-R–targeted tumor imaging. These qualities could be confirmed for [^{99m}Tc]Demogastrin 2, which provided excellent delineation of tumor deposits in a first patient with metastatic medullary thyroid cancer.

Key Words: tetraamine-peptides; cholecystokinin-2/gastrin-receptor; tumor targeting; ^{99m}Tc-labeled minigastrin

J Nucl Med 2005; 46:1727–1736

The advent of radiolabeled somatostatin analogs in the targeted imaging and radionuclide therapy of tumors overexpressing somatostatin receptors has paved the way for other radiopeptides to target alternative cancer-associated peptide receptor systems (*1–4*). Interest in this direction has been recently stimulated by reports on the high incidence (>90%) and high-density expression of CCK-2/gastrin-R (CCK-2/gastrin-R = cholecystokinin subtype 2/gastrin receptor) in human medullary thyroid cancer (MTC), already suspected by the highly sensitive pentagastrin diagnostic test (*5–7*). Of particular clinical relevance is the independence of CCK-2/gastrin-R status on the degree of tumor differentiation in human MTCs (*5,6*), whereas, in advanced and clinically aggressive forms of the disease, somatostatin receptor expression is lacking (*7,8*). The presence of CCK-2/gastrin-R has been documented in other human tumors as well, such as in small cell lung cancer (*9–11*), astrocytomas, stromal ovarian tumors, gastroenteropancreatic neuroendocrine tumors, and in extremely high densities in gastrointestinal stromal tumors (*9,12,13*), whereas the role of gastrin, CCK, and their receptors (CCK-2/gastrin-R or CCK-1-R) in gastric and colon cancer is still controversial (*9,14,15*).

In view of the above, several investigators have been involved in the development of radiolabeled gastrin/CCK analogs for targeted diagnostic imaging and radionuclide therapy of CCK-2/gastrin-R–expressing tumors. Already in the late 1990s, Behr et al. (*16*) were able to show promising results for the diagnostic and therapeutic application of ^{131}I-radioiodinated human gastrin-I. At the same time, Reubi et al. (*17*) developed a series of nonsulfated CCK(26–33) analogs coupled at the N-terminus to diethylenetriaminepentaacetic acid (DTPA) and 1,4,7,10-tetraazacyclododecane-1,4,7,10-tetraacetic acid (DOTA) for radiometal binding. Although some of these analogs originally showed promising results in rats (*18*), none displayed convincing accumulation in the strongly receptor-positive stomach or detected small lesions in MTC patients (*19*).

As nonsulfated gastrin derivatives were shown to be more suitable for tumor targeting by virtue of their CCK-2 recep-

Received Mar. 15, 2005; revision accepted Jun. 27, 2005.

For correspondence or reprints contact: Berthold A. Nock, PhD, Institute of Radioisotopes–Radiodiagnostic Products, National Center for Scientific Research Demokritos, 153 10 Ag. Paraskevi Attikis, Athens, Greece.

E-mail: nockb@rrp.demokritos.gr

tor selectivity, high affinity, and favorable in vivo profile (*20*), Behr et al. developed [^{111}In-DTPA^0]minigastrin showing high uptake in stomach and tumor lesions in metastatic MTC patients (*20*). Coupling of DTPA to [DGlu^1]-minigastrin (*21*) and of bifunctional DTPA to nonsulfated CCK8 (*22*) further improved in vivo profiles, so that the first data from the application of [^{90}Y-DTPA^0,(D)Glu^1]-minigastrin in the therapy of advanced metastatic MTC was reported soon afterward (*23*).

These developments motivated the search for a ^{99m}Tc-based CCK-2/gastrin-R–targeting radiotracer, given that ^{99m}Tc is the label of choice in diagnostic nuclear medicine (*24*). Besides its ideal nuclear characteristics, ^{99m}Tc is easily accessible at a low cost because of the availability of commercial ^{99}Mo/^{99m}Tc generators (*24*). So far, PN_2S chelators (*25*), hydrazinonicotinic acid (HYNIC) combined to different coligands (*26,27*), and tricarbonyl/N_2O-tridentate donor atom sets (*27*) have been coupled to either CCK or gastrin to enable labeling with ^{99m}Tc.

Our group has been engaged in derivatizing peptides with open-chain tetraamines to achieve stable binding of ^{99m}Tc. This approach has been successful in providing somatostatin and bombesin analogs suitable for targeted imaging applications in animals (*28,29*) and, most importantly, in humans (*30*). In the present work, we coupled this chelator system to the N-terminus of [(D)Glu^1]minigastrin either directly or via different spacers, thereby generating 3 peptide conjugates, Demogastrin 1–3. Labeling with ^{99m}Tc and study of resulting radiopeptides in cells and animal models are presented. The initial results in a metastatic MTC patient are also reported, revealing their suitability to image CCK-2/gastrin-R–expressing tumors in humans.

MATERIALS AND METHODS

Reagents and Instrumentation

Chemicals of reagent grade were used without further purification. Rink amide 4-methylbenzydrylamine (MBHA) resin and N_α-Fmoc (9-fluorenylmethoxycarbonyl)amino acids with Boc (butoxycarbonyl)–protected lateral chains were purchased from NovaBiochem AG. Physiologic saline solution containing [^{99m}Tc]$NaTcO_4$ was eluted from a commercial ^{99}Mo/^{99m}Tc generator (Tyco Healthcare) and served as a ^{99m}Tc source. For carrier-added experiments, $NH_4{}^{99g}TcO_4$ (Oak Ridge National Laboratories) was used (*28*). High-performance liquid chromatography (HPLC)–grade solvents were filtered through 0.22-μm membranes (Millipore) and degassed by helium flux before use. Instant thin-layer chromatography (ITLC) was conducted on ITLC-SG strips from PALL Life Sciences (PALL Corp.).

Solid-phase peptide synthesis was performed on a Rink Switch 24 peptide synthesizer (RinkCombichem Technologies). Chemical reactions were monitored by thin-layer chromatography (TLC) on Merck plates precoated with silica gel 60 F_{254} (0.25 mm). Preparative HPLC was performed on a Bischof HPLC system (Metrohm AG) with HPLC-pumps 2250 and a tunable Lambda 1010 ultraviolet (UV) detector (Metrohm AG) set at 280 nm. Purifications were conducted on a Machery–Nagel VP 250/21 Nucleosil 100-5 C_{18} column (21 × 250 mm) eluted at 15 mL/min flow rate by the following gradient system: 0 min 25% B, 25 min 50% B, 30 min 50% B, 31 min 100% B, 36 min 100% B, and 37 min back to 25% B, where A = 0.1% trifluoroacetic acid (TFA) in H_2O and B = acetonitrile. Electrospray ionization (ESI) mass spectroscopy (MS) was performed on a Finnigan SSQ 7000 spectrometer. Matrix-assisted laser desorption ionization (MALDI) MS was performed on a Voyager sSTR instrument (Applied Biosystems). ESI-MS spectra of [Re^V]Demogastrin 3 were taken on an LCQ (ThermoFinnigan) ion trap instrument. Analytic HPLC was performed on a Hewlett Packard 1050 HPLC system connected to a multiwavelength UV detector set to 214 nm. A Machery–Nagel Nucleosil 120-3 C_{18} column was used as stationary phase, whereas the eluent system consisted of 0.1% TFA in H_2O (solvent A) and acetonitrile (solvent B) applying the following gradient protocol at a 0.75 mL/min flow rate: 0 min 20% B, 20 min 40% B (system 1).

Chromatographic analyses of peptides were performed on a Waters system based on a 600 solvent delivery pump coupled to a twin-detector unit comprising a Waters 996 PDA UV detector and a Raytest Gabi γ-detector (Raytest GmbH). System 2: XTerra RP-8 (5 μm, 4.6 × 150 mm) analytic cartridge column (Waters) eluted at 1 mL/min with the following gradient system: 0%–40% B in 40 min, with A = 0.1% TFA in H_2O and B = acetonitrile; system 3: Symmetry Shield RP18 (5 μm, 3.9 × 150 mm) analytic cartridge column (Waters) eluted at 1 mL/min with the following gradient system: 0%–40% B in 40 min, with A = 0.2% H_3PO_4 neutralized to pH 7 with 25% aq. NH_3. Radioactivity measurements were conducted in an automated well-type γ-counter [NaI(Tl) crystal Auto-γ-5000 instrument (Canberra Packard Central Europe GmbH)]. For binding experiments, a Brandel M-48 Cell Harvester was used (Adi Hassel Ingenieur Büro).

The acinar rat pancreatic carcinoma AR4-2J cell line was kindly provided by Dr. Ralf Kleene (Philipps University, Marburg, Germany). Culture media were supplied by Gibco BRL, Life Technologies, and supplements were purchased from Biochrom KG Seromed. The protein microdetermination kit (procedure no. P5656) by Sigma-Diagnostics was used for protein measurements. In-house male Swiss albino mice (30 ± 5 g) and female Swiss *nu/nu* mice from Charles River Laboratories were used for biodistribution. Animal experiments were conducted in compliance with national and European guidelines and protocols were approved by local authorities.

Synthesis of Bioconjugates

Peptide conjugates were assembled at a 20-μmol scale on a semiautomatic peptide synthesizer using the Rink amide MBHA resin (0.6 mmol/g) following standard Fmoc solid-phase peptide synthesis. N_α-Fmoc amino acids (80 μmol) were activated in situ with a 1:1 mixture of *N*-hydroxylbenzotriazole (HOBt) and *N,N′*-diisopropylcarbodiimide (DIC). To the resin-immobilized amino acid chain R-(D)Glu-Glu-Glu-Glu-Glu-Glu-Ala-Tyr-Gly-Trp-Met-Asp-Phe-NH_2 (*R* = H or Gly), the corresponding tetraamine chelator precursor *N,N′,N″,N‴*-tetra-(tert-butoxycarbonyl)-6-X-1,4,8,11-tetraazaundecane (X = carboxy or X = *p*-[(carbomethoxy)acetyl]aminobenzyl) was coupled following the same procedure as for the addition of an amino acid residue. Cleavage of the tetraamine-peptide conjugates and deprotection were accomplished by treatment with a cocktail of thioanisole, triisopropylsilane, water, and TFA in a 5:5:5:85 (v/v/v/v) ratio for 3 h at room temperature. The crude peptides were precipitated into cold isopropylether/petroleum ether, 1:1 (v/v) mixture, and purified by preparative HPLC under the conditions given above. The desired

fractions were collected and eluents were removed on a SpeedVac apparatus. After lyophilization, pure white solids of ≥99% purity were collected. ESI-MS spectra were consistent with the expected formulae (Table 1). Overall yields were 30% for Demogastrin 1 and 2 and 10% for Demogastrin 3 based on the removal of the first Fmoc group.

Radiolabeling with ^{99m}Tc

For ^{99m}Tc labeling (*28,29*), $^{99m}TcO_4^-$ eluate (420 μL, 370–740 MBq) was transferred in an Eppendorf vial. Fifty microliters of a 0.5 mol/L Na_2HPO_4, pH 11.5–12, buffer was added, followed by 0.1 mol/L citrate solution (5 μL), 10^{-3} mol/L Demogastrin 1–3 stock solution (15 μL, 15 nmol), and a freshly prepared solution of $SnCl_2 \cdot 2H_2O$ in ethanol (15 μL, 30 μg, 157 nmol). After a 30-min incubation at room temperature, the mixture pH was adjusted to 7.4 by addition of 1 mol/L HCl. For saturation binding assays, the corresponding [^{99m}Tc/^{99g}Tc]Demogastrin 1–3 peptides were prepared according to a published protocol (*28,29*).

The isostructural *trans*-$[Re^V(O)_2(N_4)]^{+1}$ species of [^{99m}Tc]Demogastrin 1–3 (*31–34*) were prepared by reaction of Demogastrin 1–3 with excess of $[(n\text{-}C_4H_9)_4N][Re^VOCl_4]$ precursor in MeOH in the presence of *N*-ethyldiisopropylamine. All peptide present was transformed to a single species, [Re^V]Demogastrin 1–3, purified by HPLC and characterized by MALDI-TOF. Retention times of the Re and ^{99m}Tc analogs were compared by HPLC coupled to parallel UV/Vis and radiometric detection modes (Table 2).

Quality Control

Formation and radiochemical purity of [^{99m}Tc]Demogastrin 1–3 were monitored by a combination of HPLC and ITLC methods (*28*). For HPLC analyses, systems 2 and 3 were applied (Table 2). For ITLC, strips were spotted at the origin by aliquots of radiolabeled product, developed, and analyzed as previously described (*28*). Samples from the open labeling reaction vial were analyzed over a 24-h time span.

Cell Culture

CCK-2/gastrin-R–expressing AR4-2J cells (*35*) were grown to confluence in F-12 K nutrient mixture, supplemented with 10% (v/v) heat-inactivated fetal bovine serum, 1 mmol/L glutamine, 100 U/mL penicillin, and 100 μg/mL streptomycin, in humidified air containing 5% CO_2 at 37°C. A trypsin/ethylenediaminetetraacetic acid (0.05%/0.02%, w/v) solution was used for weekly passages.

Saturation Binding Assays

Saturation binding assays with [^{99m}Tc/^{99g}Tc]Demogastrin 1–3 were conducted in AR4-2J cell membranes. Membranes were obtained as previously described (*28*). For the saturation binding experiment, HPLC-purified [^{99m}Tc/^{99g}Tc]peptides were used in 2 sets of triplicates of 0.06–12 nmol/L concentration alone (total binding series) or in the presence of 1 μmol/L [(D)Glu^1]-minigastrin (nonspecific binding series) and the assay was performed according to a reported method (*28*).

Internalization

For internalization experiments, AR4-2J cells were seeded at a density of 8×10^5 cells per well in 6-well plates and grown to confluency ($1–1.5 \times 10^6$ cells per well) for 48 h. They were washed twice with ice-cold internalization medium (F-12 K nutrient mixture supplemented by 1% [v/v] fetal bovine serum) and internalization was conducted according to a published protocol (*28*). To determine nonspecific internalization, triplicates were incubated in the presence of 1 μmol/L [(D)Glu^1]minigastrin.

Metabolic Studies

Radiopeptide Stability in Murine Plasma. Blood (~1 mL) from the heart of a mouse under a mild ether anesthesia was collected in a heparinized syringe and the plasma was isolated by slight centrifugation at 4°C. For the stability experiment, samples of [^{99m}Tc]Demogastrin 1–3 were incubated with plasma at 37°C. Incubated aliquots at 15-, 30-, 60-, and 120-min time points were collected and treated with ethanol in a 1:2 (v/v) aliquot-to-ethanol ratio. After centrifugation, supernatant samples were analyzed by HPLC (system 3).

Radiopeptide Degradation in Mouse Kidney Homogenates. Swiss albino mice were anesthetized with Et_2O inhalation and their kidneys were excised, rapidly rinsed, and placed in chilled buffer, pH 7.4 (50 mmol/L Tris/0.2 mol/L sucrose), in a 1:2 (v/v) organ-to-buffer ratio. The organs were homogenized in this medium by an Ultra-Turrax T25 homogenator for 1 min at 4°C. Samples of [^{99m}Tc]Demogastrin 1–3 were incubated at 37°C in fresh homogenate and incubated aliquots at 15-, 30-, and 60-min time intervals were withdrawn and treated with ethanol in a 1:2 (v/v) aliquot-to-

TABLE 1
Analytic Data for Demogastrin Peptide-Conjugates

Peptide	Formula	MW/ES-MS (%)	HPLC t_R (min)		
			System 1*	System 2†	System 3‡
Demogastrin 1	$[N_4^0,(D)Glu^1]MG$	1,848.98/1,848.7 (100)	18.0	14.8	27.4
Demogastrin 2	$[N_4^{0-1},Gly^0(D)Glu^1]MG$	1,906.03/1,905.8 (100)	18.9	17.9	27.2
Demogastrin 3	$[N'_4{}^0,(D)Glu^1]MG$§	2,026.18/2,026.9 (100)	19.8	18.6	28.1

*System 1 = Machery–Nagel Nucleosil 120-3 C_{18} column eluted at a 0.75 mL/min flow rate with: 0 min 20% B, 20 min 40% B (A = 0.1% TFA in H_2O, B = acetonitrile).

†System 2 = XTerra RP-8 (5 μm, 4.6 × 150 mm) analytic cartridge column eluted at 1 mL/min with: 0%–40% B in 40 min (A and B as in system 1).

‡System 3 = Symmetry Shield RP18 (5 μm, 3.9 × 150 mm) analytic cartridge column eluted at 1 mL/min with: 0%–40% B in 40 min (A = 0.2% H_3PO_4 neutralized to pH 7 with 25% aq. NH_3).

§N'_4 = $(H_2NCH_2CH_2NHCH_2)CH$-(*p*-$CH_2C_6H_4$)-$NHCOCH_2OCH_2CO$-.

MW = molecular weight; MG = minigastrin.

TABLE 2
Analytic Data for (Radio)metallated Peptide-Conjugates

Peptide	Formula	MW MALDI-TOF (%, m/z)	HPLC t_R (min) System 2*	HPLC t_R (min) System 3†
[^{99m}Tc]Demogastrin 1	[^{99m}Tc]$_2N_4^0$,(D)Glu^1]MG	nd	16.7	27.1
[Re^V]Demogastrin 1	[$ReO_2N_4^0$,(D)Glu^1]MG	2,065.9 2,088.0 (100, $[M+Na]^+$)	16.0	nd
[^{99m}Tc]Demogastrin 2	[$^{99m}TcO_2N_4^{0-1}$,Gly^0(D)Glu^1]MG	nd	20.8	26.9
[Re^V]Demogastrin 2	[$ReO_2N_4^{0-1}$,Gly^0(D)Glu^1]MG	2,123.0 2,208.0 (100, $[M+2Na+K]^+$)	20.2	nd
[^{99m}Tc]Demogastrin 3	[^{99m}Tc]$_2N'_4{}^0$,(D)Glu^1]MG‡	nd	21.3	27.6
[Re^V]Demogastrin 3	[$ReO_2N'_4{}^0$,(D)Glu^1]MG	2,243.0§ 2,242.0	21.6	nd

*System 2 = XTerra RP-8 (5 μm, 4.6 × 150 mm) analytic cartridge column eluted at 1 mL/min with: 0%–40% B in 40 min A (A = 0.1% TFA in H_2O, B = acetonitrile).

†System 3 = Symmetry Shield RP18 (5 μm, 3.9 × 150 mm) analytic cartridge column eluted at 1 mL/min with: 0%–40% B in 40 min (A = 0.2% H_3PO_4 neutralized to pH 7 with 25% aq. NH_3).

‡N'_4 = $(H_2NCH_2CH_2NHCH_2)CH$-(*p*-$CH_2C_6H_4$)-$NHCOCH_2OCH_2CO$-.

§ES-MS spectra were conducted.

MW = molecular weight; MG = minigastrin; nd = not done.

ethanol ratio. After centrifugation, supernatant samples were analyzed by HPLC (system 3).

Detection of Radiometabolites in Mouse Urine. A 100-μL bolus containing >7.4 MBq [^{99m}Tc]Demogastrin 1–3 was injected in the tail vein of Swiss albino mice. Animals were kept in metabolic cages for 30 min with free access to water. They were then sacrificed by cardiac puncture while under an Et_2O anesthesia and urine was collected from their bladder with a syringe and combined with the urine collected in the cages. This urine was filtered through a Millex GV filter (0.22 μm) and aliquots of urine were treated as described above and analyzed by HPLC (system 3).

Biodistribution in Mice

Experiments in Healthy Mice. For biodistribution studies, healthy male Swiss albino mice were injected through the tail vein with a 100-μL bolus of 148–185 kBq [^{99m}Tc]Demogastrin 1–3 containing ~10 pmol total peptide. Mice were sacrificed in groups of 4 at 30 min, 1, 2, and 4 h after injection by cardiac puncture while under a slight ether anesthesia. A separate group sacrificed at 1 h after injection received 250 μg [(D)Glu^1]minigastrin together with tested radiopeptide (blocked animals). Samples of blood and urine as well as organs of interest were collected, weighed, and measured for radioactivity in a γ-counter. Intestines were not emptied of their contents. Data were calculated as percentage injected dose per gram tissue (%ID/g) using standard solutions, and statistical analysis was performed using the Student *t* test.

Experiments in AR4-2J Tumor-Bearing Nude Mice. Palpable tumor masses were grown 10 d after inoculation of a 0.8–1 × 10^7 AR4-2J cell suspension in phosphate-buffered saline (150 μL end volume) in the flanks of athymic mice. [^{99m}Tc]Demogastrin 1–3 were injected and biodistribution was performed as described. Groups of 4 animals were sacrificed at 1 and 4 h after injection, while a separate group of the 4-h time interval received 250 μg [(D)Glu^1]minigastrin together with the radioligand (blocked animals).

First Clinical Experience

For initial clinical studies, a 50-y-old patient with MTC metastatic to lymph nodes, lungs, and bone was injected with 370 MBq [^{99m}Tc]Demogastrin 2 (15 nmol of total peptide). Whole-body scans were acquired at 1.5, 4, and 24 h after injection. A double-head camera (eCam; Siemens International) equipped with a low-energy, parallel-hole collimator was used for image acquisition (45-min scanning time).

RESULTS

Radiotracers

Reduction of $^{99m}TcO_4^-$ by $SnCl_2$ in the presence of citrate anions in alkaline medium and nanomole amounts of tetraamine-coupled minigastrins produced high-purity [^{99m}Tc]Demogastrin 1–3 radiopeptides (Fig. 1) in >97% labeling yields. Single-species radiopeptide formation and absence of radiochemical impurities ($^{99m}TcO_4^-$ or ^{99m}Tc-citrate) were shown for [^{99m}Tc]Demogastrin 1–3 during HPLC analysis. The percentage of reduced, hydrolyzed ^{99m}Tc ($^{99m}TcO_2{\cdot}H_2O$) was always found to be <2%–3% during ITLC analysis. Chromatographic comparison of [^{99m}Tc]Demogastrin 1–3 with the corresponding ReO_2-authentic samples ([Re^V]Demogastrin 1–3) (Table 2) was consistent with the formation of isostructural species (Fig. 1), as previously reported for other 1,4,8,11-tetraazaundecane ^{99m}Tc/^{99g}Tc/Re-chelates (*31–34*). Radiopeptides remained intact in the open reaction vial for at least 6 h after labeling.

Receptor-Binding Studies

Saturation binding assays for [^{99m}Tc/^{99g}Tc]Demogastrin 1–3 were performed in AR4-2J cell membranes. Addition of "carrier" ^{99g}Tc provided sufficient mass of metallated conjugate for the assay (*28*). The dissociation constant (K_d) values were found to be comparable for the 3 peptides with

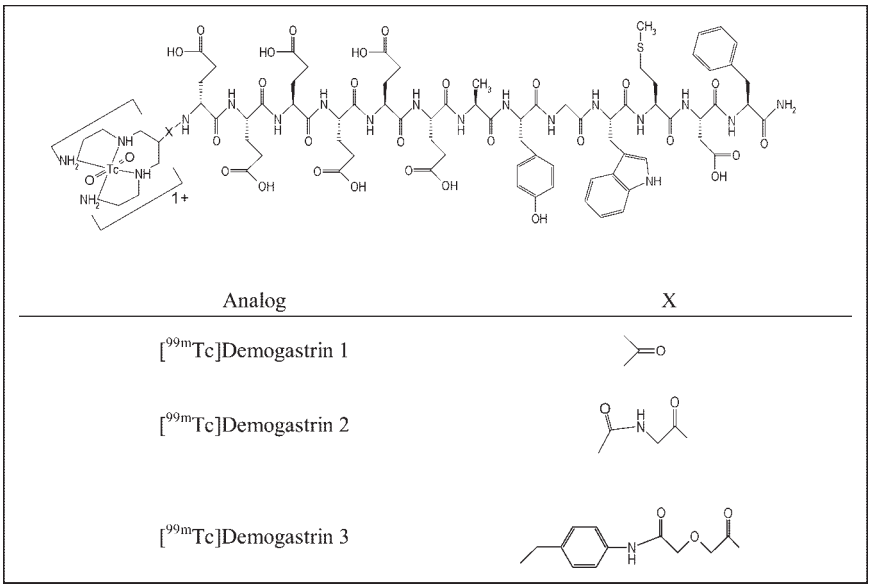

FIGURE 1. [^{99m}Tc]Demogastrin 1–3.

1.05 ± 0.13 nmol/L for [^{99m}Tc/^{99g}Tc]Demogastrin 1, 1.02 ± 0.07 nmol/L for [^{99m}Tc/^{99g}Tc]Demogastrin 2, and 1.01 ± 0.09 nmol/L for [^{99m}Tc/^{99g}Tc]Demogastrin 3. These values are lower than those reported for other ^{99m}Tc-labeled minigastrins (e.g., 10.3 nmol/L for ^{99m}Tc-EDDA/HYNIC-minigastrin) determined in the same cell line (*27*) and illustrate the high affinity of [^{99m}Tc/^{99g}Tc]Demogastrin 1–3 for the CCK-2/gastrin-R. A representative saturation curve for [^{99m}Tc/^{99g}Tc]Demogastrin 2 is presented in Figure 2.

Internalization

Time-dependent internalization curves of [^{99m}Tc/^{99g}Tc]Demogastrin 1–3 in AR4-2J cells are presented in Figure 3, revealing a rapid endocytosis of radioactivity at 37°C. An 80%–90% internalization plateau is reached within 15–30 min of incubation. In the presence of excess [(D)Glu^1]-minigastrin (1 μmol/L), internalization was reduced to ~10%, suggesting a CCK-2/gastrin-R–mediated process (*35*).

Metabolic Studies

During incubation in fresh mouse plasma at 37°C, [^{99m}Tc]Demogastrin 1–3 remained intact for at least 2 h (Fig. 4A). In contrast, analysis of mouse urine collected 30 min after administration showed no trace of original radiopeptide. Instead, radioactivity was excreted in the form of hydrophilic metabolite(s), as shown in Figure 5B for the urine analysis of [^{99m}Tc]Demogastrin 2. The metabolic product(s) found in mouse urine eluted at different retention times (t_R) than $^{99m}TcO_4^-$. Similarly, ITLC analysis of urine performed in parallel failed to reveal any trace of $^{99m}TcO_4^-$. These

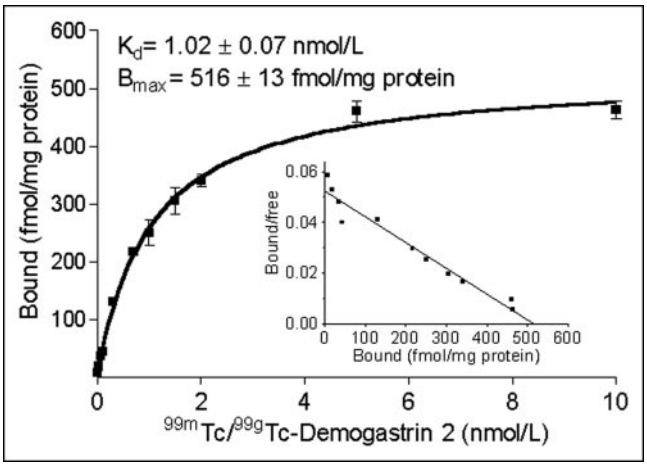

FIGURE 2. Saturation binding curve of [^{99m}Tc/^{99g}Tc]Demogastrin 2 in AR4-2J cell membranes with Scatchard plot in inset. K_d = 1.024 ± 0.07 nmol/L; B_{max} = 516 ± 13 fmol/mg protein (B_{max} is maximum number of binding sites).

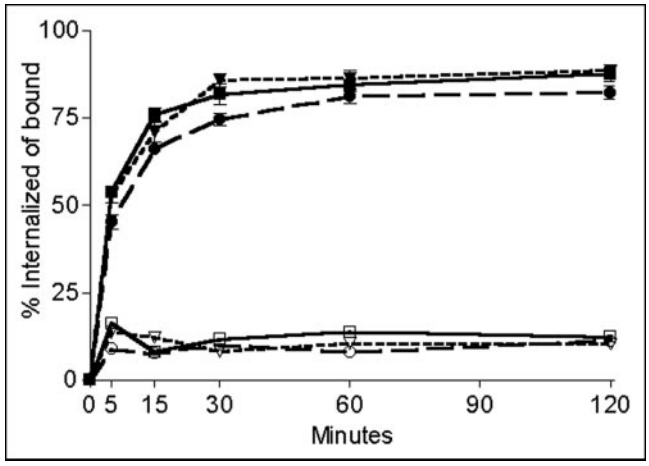

FIGURE 3. Time-dependent internalization of [^{99m}Tc]Demogastrin 1–3 in CCK-2/gastrin–expressing AR4-2J cells at 37°C in absence (filled symbols: specific) or presence (open symbols: nonspecific) of competing (10^{-6} mol/L) [(D)Glu^1]minigastrin: ■, □, [^{99m}Tc]Demogastrin 1; ●, ○, [^{99m}Tc]Demogastrin 2; and ▼, ▽, [^{99m}Tc]Demogastrin 3.

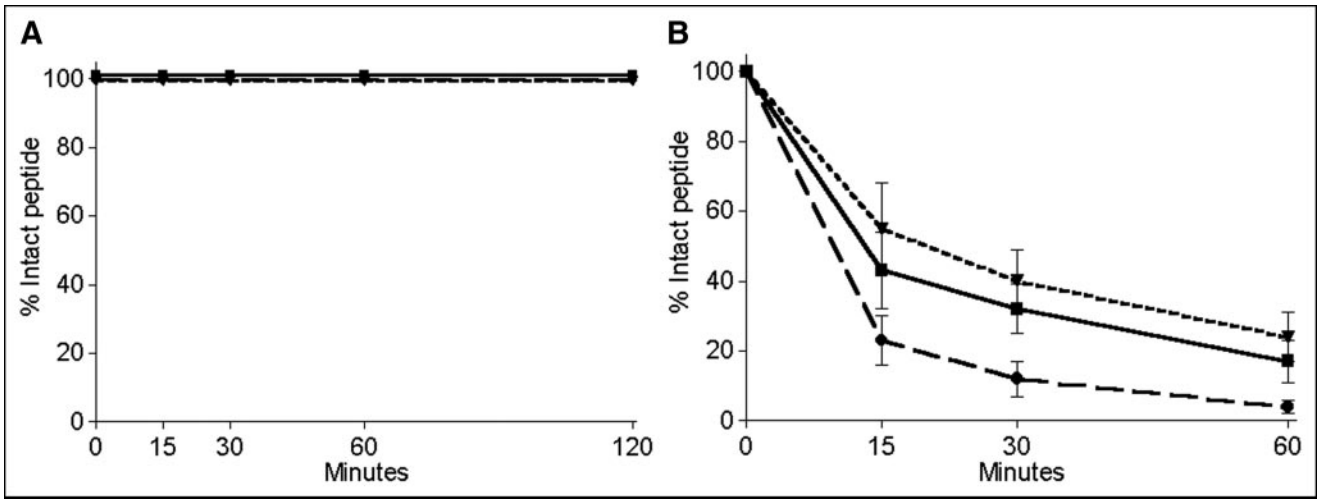

FIGURE 4. Degradation rates of [^{99m}Tc]Demogastrin 1–3 in murine plasma (A) and in mouse kidney homogenates (B): ■, [^{99m}Tc]Demogastrin 1; ●, [^{99m}Tc]Demogastrin 2; and ▼, [^{99m}Tc]Demogastrin 3.

findings are in agreement with previous studies reporting on the in vivo stability of $[^{99m}Tc(O)_2(N_4)]^+$ metal chelates in rodents (*33*) and of ^{99m}Tc-labeled tetraamine-modified somatostatin analogs in rodents and humans (*28,30*). Thus, metabolite(s) of [^{99m}Tc]Demogastrin 1–3 in urine seem to form by cleavage of peptide bond(s) either within the peptide backbone or between peptide and metal chelate. Given that the bulk of the radioactivity is sequestered via the

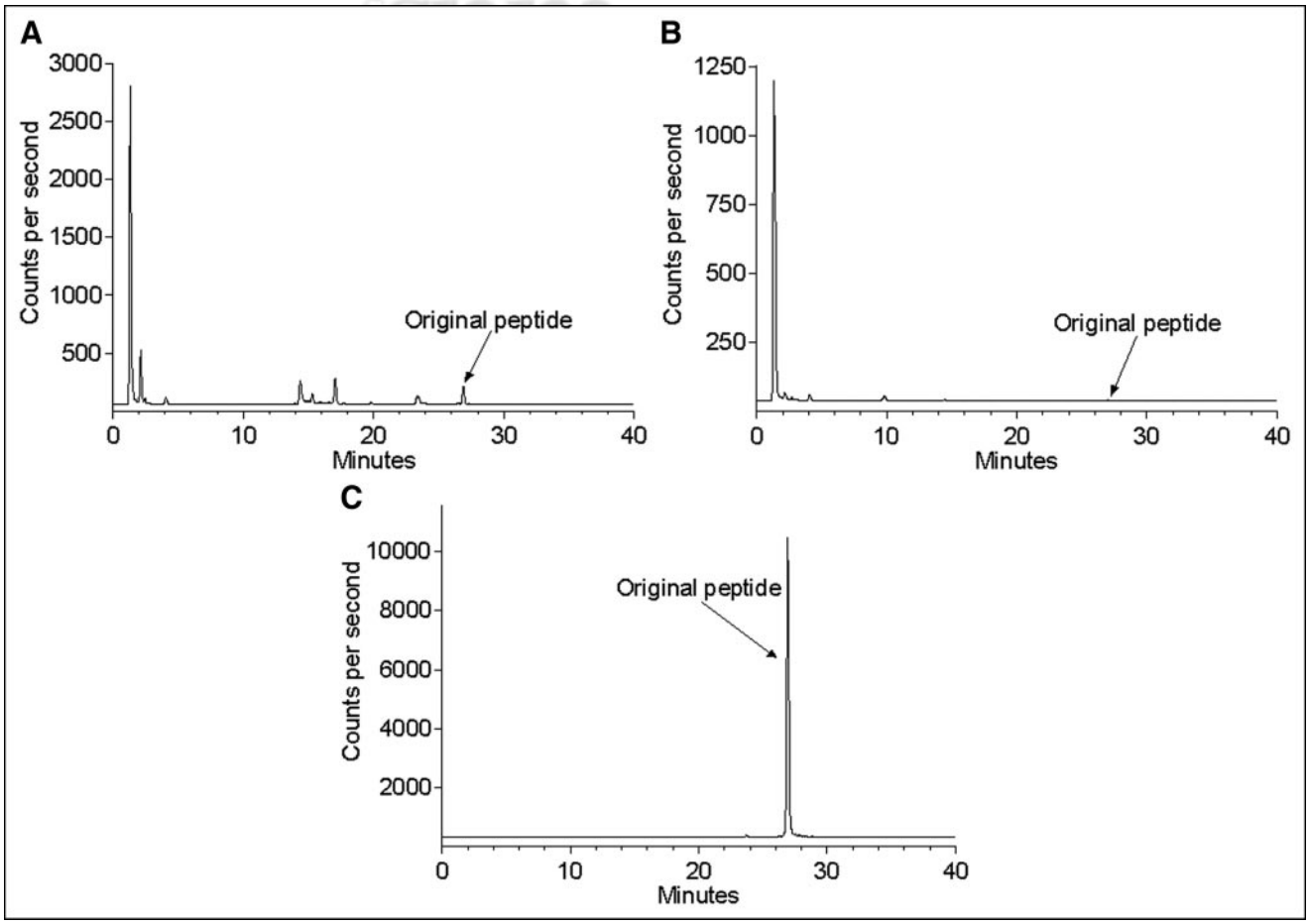

FIGURE 5. γ-Trace from HPLC analysis of [^{99m}Tc]Demogastrin 2 after 2-h incubation at 37°C in kidney homogenates (A) in urine collected 30 min after intravenous injection of radiopeptide in mice (B) and reference [^{99m}Tc]Demogastrin 2 after labeling (C).

kidneys (vide infra) and no intact radiopeptides are detected in the urine, the kidneys seem to be a major degradation site of [^{99m}Tc]Demogastrin 1–3 in mice. Indeed, during incubation of [^{99m}Tc]Demogastrin 1–3 in mouse kidney homogenates, all 3 radiopeptides were rapidly degraded to hydrophilic products with the following rank of stability: [^{99m}Tc]Demogastrin 3 $\geq$ [^{99m}Tc]Demogastrin 1 $>$ [^{99m}Tc] Demogastrin 2 (Fig. 4B). The main metabolites were eluting with the same t_R as those detected in mouse urine. In addition, several minor metabolite intermediate peaks were also detected, as shown in the representative radiochromatogram of 2-h mouse kidney incubates of [^{99m}Tc]Demogastrin 2 in Figure 5A.

Animal Studies

Biodistribution in Healthy Mice. Selective data of [^{99m}Tc] Demogastrin 1–3 biodistribution in healthy mice are summarized for comparison in Figure 6. Results are given as %ID/g and include the stomach (Fig. 6A), as the main site of natural CCK-2/gastrin-R expression, as well as the kidneys (Fig. 6B) and liver (Fig. 6C). [^{99m}Tc]Demogastrin 1–3 exhibited a high and rapid localization at the target organ of ~3 %ID/g at 30 min after injection. Uptake in the stomach could be blocked by >85% at 1 h after injection by coinjection of 250 μg [(D)Glu^1]minigastrin with each radiopeptide, suggesting a receptor-specific process. Values in the stomach declined slowly to about 1.5 %ID/g at 4 h after injection (Fig. 6A).

Radioactivity was excreted predominantly via the kidneys, with a low percentage processed via the liver. Kidney values were lower for [^{99m}Tc]Demogastrin 3, which instead showed a higher portion of liver activity, most probably because of the presence of an extra aromatic ring in the spacer increasing the lipophilicity of this particular compound. It is interesting to note that coinjection of excess [(D)Glu^1]minigastrin provoked a 50% reduction in the kidney uptake ($P < 0.001$). The same effect was observed by coinjection of the respective amount of (D)Glu-$(Glu)_5$ peptide (results not shown). This finding is in agreement with data reported on the lack of CCK-2/gastrin-Rs in the kidneys and implies a poly-Glu–related uptake in the mouse kidney. Similar effects in the renal uptake of [^{111}In-DTPA^0,(D)Glu^1]minigastrin after intraperitoneal adminis-

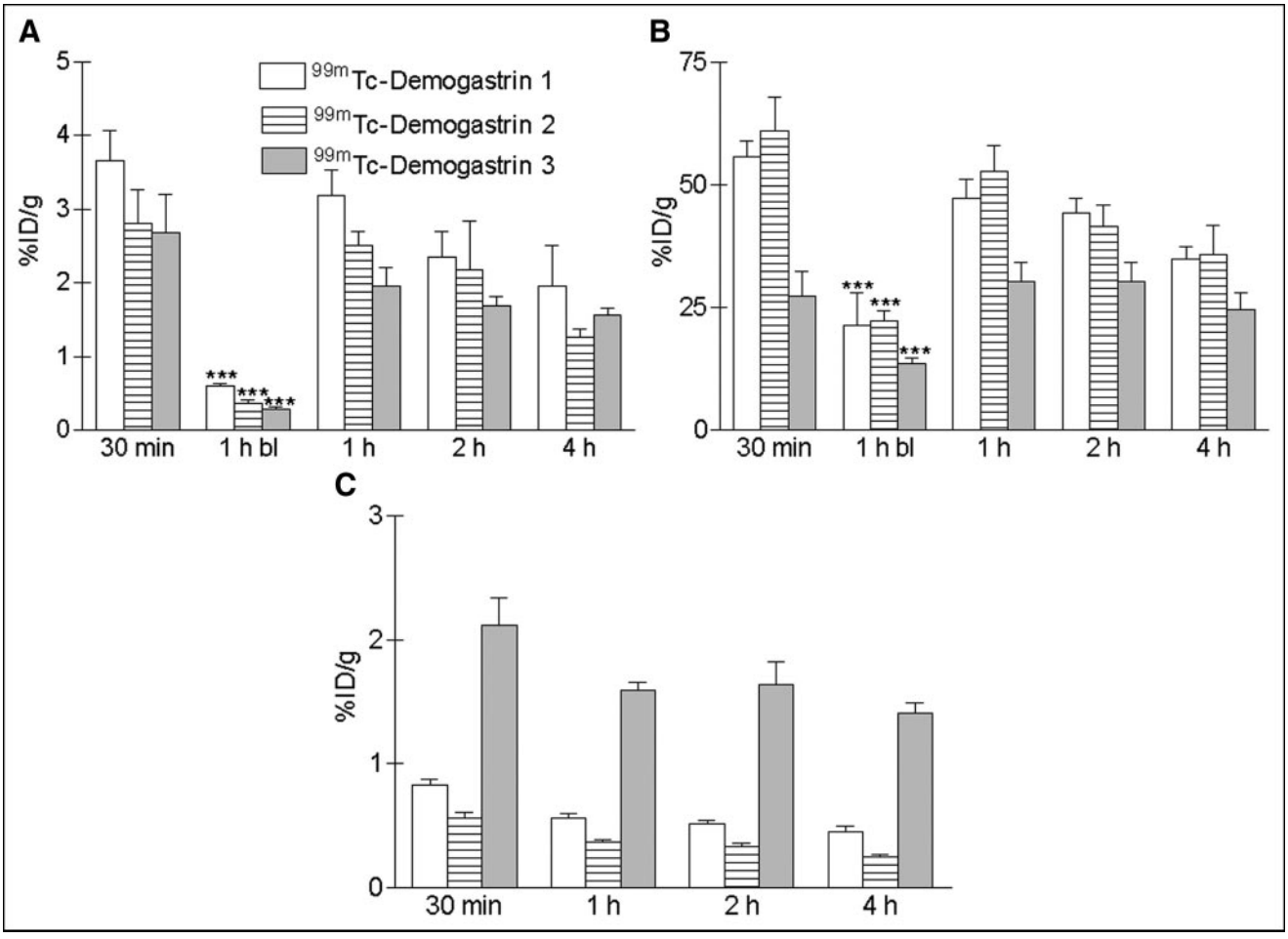

FIGURE 6. Selective data of [^{99m}Tc]Demogastrin 1–3 biodistribution in healthy mice at 30 min, 1, 2, and 4 h after injection in stomach (A), kidneys (B), and liver (C). Results are the average %ID/g values from groups of 4 animals at each time point. bl = blocked. Student *t* test was used for statistical analysis and a *P* value of <0.001 (***P) was considered extremely significant.

tration of $(Glu)_x$ ($x \geq 5$) species in tumor-bearing Lewis rats have been recently reported by Béhé et al. (*36*).

Biodistribution in AR4-2J Tumor-Bearing Mice. Data of [^{99m}Tc]Demogastrin 1–3 biodistribution in nude mice bearing AR4-2J tumors are summarized as %ID/g tissue in Table 3 for 1- and 4-h time intervals. The analogs showed a very rapid clearance from the blood and nontarget organs of mice via the kidneys. All 3 analogs were able to effectively target the CCK-2/gastrin-R–positive stomach and the experimental tumor specifically, as demonstrated by the >85% drop in the respective values found in the animals treated with an excess of [(D)Glu^1]minigastrin. The high tumor targeting and rapid background clearance attained in mice by [^{99m}Tc]Demogastrin 1–3 (Table 4) indicate their potential usefulness for CCK-2/gastrin-R–targeted tumor imaging. [^{99m}Tc]Demogastrin 1 and 2 exhibited lower liver uptake, thereby showing more promise for clinical application. However, the kidney values were still very high (75–85 %ID/g at 1 h after injection, dropping to ~42 %ID/g at 4 h after injection). Similarly to the kidney data in healthy mice, coinjection of excess [(D)Glu^1]minigastrin provoked an extremely significant reduction in the kidney values ($P < 0.001$) that exceeded 50%.

MTC Patient Imaging

The whole-body scans of a patient with metastatic MTC are shown in Figure 7. All known lesions in lymph nodes, lungs, and bone were detected already at 90 min after injection. In addition, physiologic uptake is observed in the strongly CCK receptor–positive stomach while a fast clearance via the kidneys into the bladder is clearly visible. The image 4 h after injection shows a similar distribution pattern but with more clarity because of a lower background. Thus, bone metastases are visualized with a very high resolution. The additional uptake seen in the intestines is activity released from the stomach during this period. The 24-h images have not been included. Similar to other ^{99m}Tc-based radiopeptides (*30*), the rapid radiotracer clearance and the low counting rate led to poorer quality images.

DISCUSSION

Evidence on the CCK-2/gastrin-R expression in several malignant tumors—especially MTCs—has provided the molecular basis for the development of radiolabeled CCK and gastrin analogs for targeted tumor imaging and radionuclide therapy (*6,9–15*). In fact, several research groups have been actively engaged in this effort using either CCK or gastrin motifs. Nonsulfated CCK analogs have been usually preferred over sulfated CCK compounds due to their selectivity for the CCK-2/gastrin-R (*5,9,17–19,22*). In contrast, the sulfated analogs were expected to unnecessarily raise background activity as a result of binding also to CCK-1-Rs physiologically expressed in several tissues in the body. On the other hand, gastrin-derived compounds, besides their selectivity, show also a higher affinity for the CCK-2/gastrin-R (*5,16,20,21,23*). Their major drawback, however, is their prolonged renal retention, which complicates radionuclide therapy by increasing the risk of nephrotoxicity. Nevertheless, recent results from the therapeutic application of [^{90}Y-DTPA^0,(D)Glu^1]minigastrin in metastatic MTC patients have been very promising (*23*). On the other hand, the search for a ^{99m}Tc-based radiotracer for targeted tumor imaging has been initiated with recent studies involving PN_2S-, tricarbonyl/N_2O-, or HYNIC/coligand-derivatized CCK or gastrin analogs (*25–27*).

TABLE 3
Biodistribution Data of [^{99m}Tc]Demogastrin 1–3 in AR4-2J Tumor-Bearing Athymic Mice as %ID/g Tissue (Mean ± SD)

Organ	[^{99m}Tc]Demogastrin 1		[^{99m}Tc]Demogastrin 2		[^{99m}Tc]Demogastrin 3
	1 h pi	4 h pi	1 h pi	4 h pi	1 h pi
Blood	0.36 ± 0.10	0.15 ± 0.01	0.17 ± 0.02	0.03 ± 0.00	0.35 ± 0.06
Liver	0.34 ± 0.05	1.04 ± 0.09	0.63 ± 0.20	0.38 ± 0.03	2.61 ± 0.49
Heart	0.15 ± 0.04	0.09 ± 0.02	0.30 ± 0.18	0.04 ± 0.00	0.28 ± 0.06
Kidneys	78.97 ± 1.60	41.08 ± 4.21	83.92 ± 14.45	42.65 ± 4.18	78.18 ± 11.85
Blocked kidneys	17.78 ± 0.07†	20.95 ± 1.27*	27.95 ± 6.49*	14.03 ± 1.84†	19.50 ± 3.84*
Stomach	6.59 ± 0.50	3.47 ± 0.23	5.86 ± 0.28	3.96 ± 0.26	5.96 ± 0.49
Blocked stomach	1.06 ± 0.08†	0.45 ± 0.17†	0.43 ± 0.01†	0.16 ± 0.03†	0.41 ± 0.10†
Intestine	0.62 ± 0.19	1.07 ± 0.16	0.44 ± 0.02	0.54 ± 0.04	0.37 ± 0.03
Spleen	0.17 ± 0.02	0.22 ± 0.40	0.13 ± 0.03	0.10 ± 0.01	0.33 ± 0.09
Muscle	0.12 ± 0.05	0.09 ± 0.00	0.09 ± 0.07	0.02 ± 0.01	0.12 ± 0.05
Lung	0.37 ± 0.05	0.18 ± 0.02	0.54 ± 0.29	0.06 ± 0.01	0.45 ± 0.09
Pancreas	0.28 ± 0.05	0.13 ± 0.01	0.22 ± 0.10	0.09 ± 0.02	0.23 ± 0.02
AR4-2J tumor	6.13 ± 3.28	2.70 ± 1.12	5.50 ± 0.85	2.88 ± 0.42	4.20 ± 1.22
Blocked tumor	0.94 ± 0.42*	0.34 ± 0.01*	0.45 ± 0.07†	0.17 ± 0.00†	0.52 ± 0.11*

Student *t* test was used for statistical analysis; a *P* value of <0.01 (**P*) was considered very significant, whereas a *P* value of <0.001 (†*P*) was considered extremely significant.

pi = after injection.

Results are average of 4 animals per group. Blocking was achieved by coinjection of 250 μg [(D)Glu^1]minigastrin.

TABLE 4
Tumor-to-Background Ratios After Injection of [^{99m}Tc]Demogastrin 1–3 in AR4-2J Tumor-Bearing Mice

Organ	[^{99m}Tc]Demogastrin 1		[^{99m}Tc]Demogastrin 2		[^{99m}Tc]Demogastrin 3
	1 h pi	4 h pi	1 h pi	4 h pi	1 h pi
Tumor/blood	17	18	32	96	12
Tumor/liver	18	3	9	8	2
Tumor/muscle	51	30	61	144	35
Tumor/blocked tumor	6	8	12	17	8

pi = after injection.

In this work, we present 3 new [(D)Glu^1]minigastrin analogs, Demogastrin 1–3 (Fig. 1). For ^{99m}Tc labeling, these compounds carry at their N-terminus an open-chain tetraamine (N_4) attached either directly (Demogastrin 1) or through a spacer (Demogastrin 2 and 3). The N_4 chelator has been known to generate in vivo stable complexes in specific activities suitable for receptor-targeting applications (*33*). Our own experience with this system has been very positive in providing ^{99m}Tc-labeled somatostatin and bombesin analogs with promise for clinical application (*28–30*). Furthermore, the formation of isostructural technetium and rhenium complexes with this chelator (*31–34*) provides the exciting possibility to eventually develop the respective ^{188}Re-based therapeutic agents (*34*).

During labeling [^{99m}Tc]Demogastrin 1–3 were easily accessible in >98% purity and specific activity of ~37 GBq/μmol. Coelution of [^{99m}Tc]Demogastrin 1–3 (γ trace) with authentic Re^V samples (UV/visible trace) verified the formation of the [$^{99m}Tc^V(O)_2(N_4)]^+$-peptide species (Table 2). The (radio)metallated peptide conjugates exhibited high affinity for the CCK-2/gastrin-R with a K_d = ~1 nmol/L, well below previously reported values, such as ^{99m}Tc-EDDA/HYNIC-minigastrin (10.3 nmol/L) (*27*) or ^{111}In-DTPA-Glu-G-CCK8 (20 nmol/L) (*22*), revealing that the monocationic [$^{99m}Tc^V(O)_2(N_4)]^+$-chelate favors interaction with the CCK-2/gastrin-R. In addition to their high affinity, the radiopeptides displayed rapid and receptor-mediated internalization in AR4-2J cells.

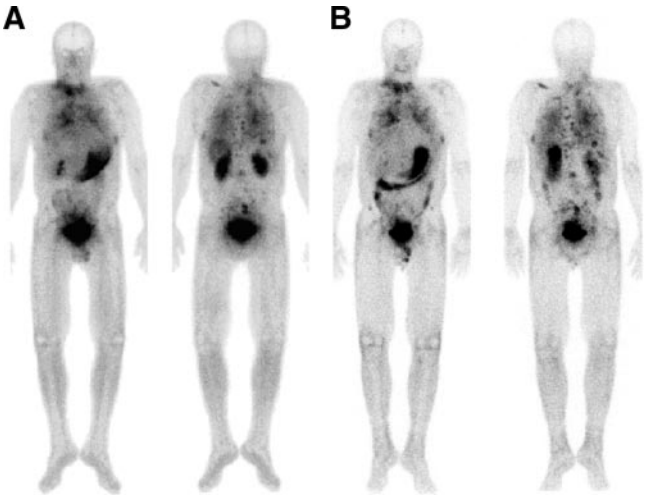

FIGURE 7. Whole-body images of patient with metastatic MTC 90 min (A) and 240 min (B) after intravenous injection of 740 MBq [^{99m}Tc]Demogastrin 2.

After injection in mice, [^{99m}Tc]Demogastrin 1–3 were cleared very rapidly from blood and nontarget tissues via the kidneys and the urinary system. The stomach—the major site of CCK-2/gastrin-R expression—showed a high and receptor-mediated uptake, demonstrating the capacity of new analogs to target this receptor in vivo. As expected for minigastrin-based analogs, a high kidney uptake was also observed, with kidney values, however, declining over time (Fig. 6B). Despite their high plasma stability, the kidneys were found to be a major site of [^{99m}Tc]Demogastrin 1–3 catabolism to hydrophilic species eventually excreted in the urine. An intriguing feature in the behavior of these peptides is the significant reduction ($P < 0.001$) in their renal uptake by coinjection of excess (250 μg) [(D)Glu^1]minigastrin (Fig. 6B) or poly-Glu–containing species. Taking into consideration the lack of CCK-2/gastrin-R expression in the kidney, this finding implies a $(Glu)_x$-related uptake mechanism in this organ and warrants further investigation. Interestingly, similar observations have been reported after intraperitoneal injection of $(Glu)_x$ species in rats and a new method for reducing renal uptake of negatively charged peptides is proposed (*36*).

In nude mice bearing AR4-2J tumors, [^{99m}Tc]Demogastrin 1–3 localized very rapidly in the stomach and in the tumor by a receptor-mediated process. Again, a high renal uptake was observed that was significantly reduced by coinjection of parent peptide. Overall the tumor-to-nontarget tissue ratios were high for all 3 analogs, but especially favorable for [^{99m}Tc]Demogastrin 2 (Table 4). Therefore, [^{99m}Tc]Demogastrin 2 was selected for further validation in a first metastatic MTC patient. The first images revealed all known lesions already at 90 min after injection. The image 4 h after injection showed a very similar radioactivity distribution with a higher contrast because of lower background activity (higher target-to-nontarget ratios) as well as uptake in the intestine caused by activity release from the stomach. The very fast blood and background clearance of minigastrin seems to be ideally matched by the physical

properties—half-life of 6 h—of ^{99m}Tc providing excellent quality images, especially at 4 h after injection.

CONCLUSION

This study has shown that coupling of a tetraamine chelator to [(D)Glu^1]minigastrin enables labeling with ^{99m}Tc with a high efficiency. The resulting peptides, [^{99m}Tc]Demogastrin 1–3, effectively interact with the CCK-2/gastrin-R both in vitro and in animal models. These promising qualities were confirmed by the excellent images obtained by [^{99m}Tc]Demogastrin 2 in a first metastatic MTC patient.

ACKNOWLEDGMENTS

The authors thank Dr. Daniel Storch (Radiology Department, Kantonsspital Basel, Basel, Switzerland) for his assistance with MALDI-TOF measurements of [Re^V]Demogastrins 1 and 2 as well as Drs. Pietro Traldi, Michela Tubaro, and Francesco Tisato (Istituto di Chimica Inorganica e delle Superfici, Consiglio Nazionale delle Ricerche, Padova, Italy) for ESI-MS measurements of [Re^V] Demogastrin 3. Assistance by the European Union through COST Action B12: "Radiotracers for In Vivo Assessment of Biologic Function", WG-3: "Radiolabeled Biologically Active Peptides" is gratefully acknowledged. Partial financial support was provided as well by Biomedica Life Sciences, S.A. Financial support was also provided by the Swiss National Science Foundation (Project 3100A0-100390).

REFERENCES

1. Breeman WAP, de Jong M, Kwekkeboom DJ, et al. Somatostatin receptor-mediated imaging and therapy: basic science, current knowledge, limitations and future perspectives. *Eur J Nucl Med Mol Imaging.* 2001;28:1421–1429.
2. de Jong M, Kwekkeboom D, Valkema R, Krenning EP. Radiolabeled peptides for tumour therapy: current status and future directions. *Eur J Nucl Med Mol Imaging.* 2003;30:463–469.
3. Reubi JC. Peptide receptors as molecular targets for cancer diagnosis and therapy. *Endocr Rev.* 2003;24:389–427.
4. Reubi JC, Mäcke HR, Krenning EP. Candidates for peptide receptor radiotherapy today and in the future. *J Nucl Med.* 2005;46(suppl 1):67S–75S.
5. Béhé M, Behr TM. Cholecystokinin-B (CCK-B)/gastrin receptor targeting peptides for staging and therapy of medullary thyroid cancer and other CCK-B receptor expressing malignancies. *Biopolymers.* 2002;66:399–418.
6. Reubi JC, Waser B. Unexpected high incidence of cholecystokinin B/gastrin receptors in human medullary thyroid carcinomas. *Int J Cancer.* 1996;67:644–647.
7. Reubi JC, Chayvialle JA, Franc B, Cohen R, Calmettes C, Modigliani E. Somatostatin receptors and somatostatin content in medullary thyroid carcinomas. *Lab Invest.* 1991;64:567–573.
8. Kwekkeboom DJ, Reubi JC, Lamberts SWJ, et al. In vivo somatostatin receptor imaging in medullary thyroid carcinoma. *J Clin Endocrinol Metab.* 1993;76:1413–1417.
9. Reubi JC, Schaer JC, Waser B. Cholecystokinin (CCK)-A and CCK-B/gastrin receptors in human tumors. *Cancer Res.* 1997;57:1377–1386.
10. Sethi T, Herget T, Wu SV, Walsh JH, Rozengurt E. CCK-A and CCK-B receptors are expressed in small cell lung cancer lines and mediate Ca^{2+} mobilization and clonal growth. *Cancer Res.* 1993;53:5208–5213.
11. Matsumori Y, Katakami N, Ito M, et al. Cholecystokinin-B/gastrin receptor: a novel molecular probe for human small cell lung cancer. *Cancer Res.* 1995;55:276–279.
12. Reubi JC, Waser B. Concomitant expression of several peptide receptors in neuroendocrine tumors as molecular basis for in vivo multireceptor tumor targeting. *Eur J Nucl Med Mol Imaging.* 2003;30:781–793.
13. Reubi JC, Korner M, Waser B, Mazzucchelli L, Guillou L. High expression of peptide receptors as a novel target in gastrointestinal stromal tumors. *Eur J Nucl Med Mol Imaging.* 2004;31:803–810.
14. Upp JR, Singh P, Townsend CM, Thompson JC. The clinical significance of gastrin receptors in human colon cancers. *Cancer Res.* 1989;49:488–492.
15. Imdahl A, Mantamadiotis T, Eggstein S, Farthmann EH, Baldwin GS. Expression of gastrin, gastrin/CCK-B and gastrin CCK-C receptors in human colorectal carcinomas. *J Cancer Res Clin Oncol.* 1995;121:661–666.
16. Behr TM, Jenner N, Radetzky S, et al. Targeting of cholecystokinin-B/gastrin receptors in vivo: preclinical and initial clinical evaluation of the diagnostic and therapeutic potential of radiolabeled gastrin. *Eur J Nucl Med.* 1998;25:424–430.
17. Reubi JC, Waser B, Schaer JC, et al. Unsulfated DTPA- and DOTA-CCK analogs as specific high-affinity ligands for CCK-B receptor-expressing human and rat tissues in vitro and in vivo. *Eur J Nucl Med.* 1998;25:481–490.
18. de Jong M, Bakker WH, Bernard BF, et al. Preclinical and intitial clinical evaluation of ^{111}In-labeled nonsulfated CCK_8 analog: a peptide for CCK-B receptor-targeted scintigraphy and radionuclide therapy. *J Nucl Med.* 1999;40:2081–2087.
19. Kwekkeboom DJ, Bakker WH, Kooij PPM, et al. Cholecystokinin receptor imaging using an octapeptide DTPA-CCK analogue in patients with medullary thyroid carcinoma. *Eur J Nucl Med.* 2000;27:1312–1317.
20. Behr TM, Jenner N, Béhé M, et al. Radiolabeled peptides for targeting cholecystokinin-B/gastrin receptor-expressing tumors. *J Nucl Med.* 1999;40:1029–1044.
21. Béhé M, Becker W, Gotthardt M, Angerstein C, Behr TM. Improved kinetic stability of DTPA-DGlu as compared with conventional monofunctional DTPA in chelating indium and yttrium: preclinical and initial clinical evaluation of radiometal labeled minigastrin derivatives. *Eur J Nucl Med Mol Imaging.* 2003;30:1140–1146.
22. Aloj L, Caracò C, Panico M, et al. In vitro and in vivo evaluation of ^{111}In-DTPAGlu-G-CCK8 for cholecystokinin-B receptor imaging. *J Nucl Med.* 2004;45:485–494.
23. Behr TM, Béhé M. Cholecystokinin-B/gastrin receptor-targeting peptides for staging and therapy of medullary thyroid cancer and other cholecystokinin-B receptor-expressing malignancies. *Semin Nucl Med.* 2002;32:97–109.
24. Liu S, Edwards DS. ^{99m}Tc-Labeled small peptides as diagnostic radiopharmaceuticals. *Chem Rev.* 1999;99:2235–2268.
25. Aloj L, Panico M, Caracò C, et al. In vitro and in vivo characterization of indium-111 and technetium-99m labeled CCK-8 derivatives for CCK-B receptor imaging. *Cancer Biother Radiopharm.* 2004;19:93–98.
26. Laverman P, Béhé M, Oyen WJG, et al. Two technetium-99m-labeled cholecystokinin-8 (CCK8) peptides for scintigraphic imaging of CCK receptors. *Bioconjugate Chem.* 2004;15:561–568.
27. von Guggenberg E, Béhé M, Behr TM, Saurer M, Seppi T, Decristoforo C. ^{99m}Tc-labeling and in vitro and in vivo evaluation of HYNIC- and (N_α-His)acetic acid-modified [D-Glu^1]minigastrin. *Bioconjugate Chem.* 2004;15:864–871.
28. Maina T, Nock B, Nikolopoulou A, et al. [^{99m}Tc]Demotate, a new ^{99m}Tc-based [Tyr^3]octreotate analogue for the detection of somatostatin receptor-positive tumours: synthesis and preclinical results. *Eur J Nucl Med Mol Imaging.* 2002;29:742–753.
29. Nock BA, Nikolopoulou A, Galanis A, et al. Potent bombesin-like peptides for GRP-receptor targeting of tumors with ^{99m}Tc: a preclinical study. *J Med Chem.* 2005;48:100–110.
30. Decristoforo C, Maina T, Nock B, Gabriel M, Cordopatis P, Moncayo R. ^{99m}Tc-Demotate 1: first data in tumour patients—results of a pilot/phase I study. *Eur J Nucl Med Mol Imaging.* 2003;30:1211–1219.
31. Mantegazzi D, Ianoz E, Lerch P, Nicolò F, Chapuis G. Preparation and crystal structure of polymeric lithium[dioxoTc(V)-tetraazaundecane]-bis(trifluoromethanesulfonate) complex. *Inorg Chim Acta.* 1990;176:99–105.
32. Parker D, Roy PS. Synthesis and characterization of stable Re(V) dioxo complexes with acyclic tetraamine ligands, $[LReO_2]^+$. *Inorg Chem.* 1988;27:4127–4130.
33. Bläuenstein P, Pfeiffer G, Schubiger PA, et al. Chemical and biological properties of a cationic Tc-tetraamine complex. *Int J Appl Radiat Isot.* 1985;36:315–317.
34. Prakash S, Went MJ, Blower PJ. Cyclic and acyclic polyamines as chelators of rhenium-186 and rhenium-188 for therapeutic use. *Nucl Med Biol.* 1996;23:543–549.
35. Svoboda M, Dupuche MH, Lambert M, Bui D, Christophe J. Internalization-sequestration and degradation of cholecystokinin (CCK) in tumoral rat pancreatic AR 4-2 J cells. *Biochim Biophys Acta.* 1990;1055:207–216.
36. Béhé M, Kluge G, Becker W, Gotthardt M, Behr T. Use of polyglutamic acids to reduce uptake of radiometal-labeled minigastrin in the kidneys. *J Nucl Med.* 2005;46:1012–1015.